



# Remote Assessment of Soil Temperature on the Example of a Carbon Landfill Site of the Republic of Bashkortostan (Yangan-Tau Geopark)

Ekaterina Bogdan<sup>1,2</sup><sup>a</sup>, Alexander Volkov<sup>1,3</sup><sup>b</sup>, Larisa Belan<sup>1,2</sup><sup>c</sup>,

Rita Kamalova<sup>1,2</sup><sup>d</sup> and Iren Tuktarova<sup>1</sup><sup>e</sup>

<sup>1</sup>Ufa State Petroleum Technological University, Ufa, Russia

<sup>2</sup>Bashkir State University, Ufa, Russia

<sup>3</sup>Vector LLC, Ufa, Russia

**Keywords:** Soil temperature, thermodynamic temperature, data loggers, Landsat, Semi-automatic classification plugin, Yangan-Tau Geopark.

**Abstract:** The article discusses approaches to remote assessment of the Earth's surface temperature (on the example of the territory of the Yangan-Tau geopark, Republic of Bashkortostan, Russia). The relevance of remote assessment of soil temperature is confirmed by studies demonstrating the high ecosystem role of this indicator. The comparison of mathematical calculations of thermodynamic temperature and data generated by the Semi-automatic classification plugin module of the Q-GIS program is carried out. The interrelations between the results of ground-based studies of soil temperature obtained using data loggers and data from the thermal channels of the Landsat 8 satellite are evaluated. The absence of a relationship between data loggers and satellite imagery data in winter is determined, which is explained by the presence of snow cover. The greatest correlation was found in the autumn period. A regression analysis was carried out, on the basis of which a model of the relationship between data from Landsat 8 satellite images and the results of measurements by data loggers of soil temperature was formed.

## 1 INTRODUCTION


Many studies show a significant influence of soil temperature on ecosystem processes. In particular, the impact of extreme soil temperature events can affect the levels of biological organization (Jentsch, Beierkuhnlein, 2008; Larjavaara et al., 2021) and interact with other driving climatic variables, changing the range and stability of many ecosystems (Thuiller et al., 2008). The influence of temperature on microbiological activity, nutrient mineralization and soil respiration is noted (Yuste et al., 2007; Hamdi et al., 2013), including short-term (12 hours) near-surface extremes of soil temperature - 30-35°C (Yuste et al., 2007), as well as soil warming from 15


up to 25°C (Kravchenko et al., 2019) significantly reduce microbial activity and soil respiration in ecosystems.


Thus, monitoring the temperature regime of the soil cover is one of the necessary conditions for measures to adapt to climate change and prepare forecasts of the dynamics of vegetation productivity.


Convenience and efficiency are demonstrated by remote methods for estimating the temperature of the Earth's surface using Landsat satellite data. In their study (El Garouani et al., 2021) showed that the surface temperature has a high correlation with the air temperature and differs only by a few degrees. In the work (Mamash et al., 2021) for the city of Novosibirsk, data obtained at meteorological stations and from Landsat satellites were compared. The

<sup>a</sup>  <https://orcid.org/0000-0003-0566-2639>

<sup>b</sup>  <https://orcid.org/0000-0001-5691-6438>

<sup>c</sup>  <https://orcid.org/0000-0003-3098-7881>

<sup>d</sup>  <https://orcid.org/0000-0002-8964-7622>

<sup>e</sup>  <https://orcid.org/0000-0003-4731-1394>

standard deviation between the temperature values ranged from 0.5 to 1.9°C. For the Republic of Tyva, according to the Landsat 8 satellite, in the winter of 2014-2017, the value of the surface temperature differs from the air temperature by an average of -1.9 °C (Kuular, 2018).

## 2 MATERIALS AND METHODS

The research is carried out on the territory of the Yangan-Tau UNESCO global geopark. One of the key positions in the geopark's activities is the implementation of Sustainable Development Goal No. 13 "Taking urgent measures to combat climate change and its consequences". In 2021, the geopark entered the program of the carbon landfill of the Republic of Bashkortostan, as one of the sites.

To identify current climatic trends occurring in the territory of the Yangan-Tau Geopark, we analyzed data from long-term observations of the Duvan meteorological station in the period 1966-2019. The basic characteristics of climatic values were calculated: average (climatic norms of 1966-2019 and 1981-2010), standard deviation for temperature and coefficient of variation for precipitation, anomalies of values (the basic norm of the period 1981-2010 was used in the calculations). The assessment of regional climate changes was obtained using trend analysis. The angular coefficient of the slope of the trend line is characterized by the rate of change of the value, and the positive sign of the coefficient indicates an increase in the value of a quantity, the negative sign indicates its decrease. The value of the determination coefficient was used to assess the contribution of the linear trend to the overall variability of the indicator and its statistical significance (Kamalova et al., 2021).

A time analysis of the thermal regime revealed that in almost all months there is an increase in air temperature. Statistically significant trends were found in January, October and for the year, as well as in March of the period 1981-2010.

The increase in air temperature also confirms the long-term course of its anomalies. Their distribution shows that the frequency of warm years has been increasing since the early 2000s. Changes are observed not only in the thermal regime of the air, but also in the moisture regime. Trend analysis shows that the annual precipitation tends to increase in the period 1966-2019 (12 mm/10 years). At the same time, considering the period of the basic norm of 1981-2010, the opposite trend is found – a decrease in the amount of precipitation at a rate of -11.6 mm/10

years. In general, the greatest contribution to this trend is made by the trendline slope coefficient of the amount of precipitation of the warm period (-24.6 mm/10 years). The amount of precipitation during the cold period has positive statistically significant trends (21.6 mm/10 years). The revealed trends of the main climatic indicators collectively affect changes in the hydrothermal conditions of the geopark territory. One of the widely used indicators is the aridity index of D. A. Pedyu (Perevedentsev et al., 2011). In the work (Kamalova et al., 2021), it was found that the long-term dynamics of the aridity index shows a tendency to increase (0.26 units/10 years). Thus, summer conditions shift towards greater aridity, which, in turn, affects the hydrothermal conditions of the soil.

Ground-based studies were conducted using CEM-DT-171, Testo and VerigoPod temperature and humidity data loggers. Packed in a container, the data logger got into the soil to a depth of 15-20 cm (Figure 1).



Figure 1: Placement of data loggers at the research site in the Yangan-Tau UNESCO global Geopark.

5 sites were selected on the territory of the geopark, where data loggers were placed (Figure 2).

2 data loggers of different brands were placed on each site to adjust the results. Studies have not shown significant discrepancies in the measurement results of data loggers from different manufacturers. The study began in November 2020. Every six months, data is read from data loggers and batteries are replaced.

Remote methods. The basis for remote analysis was Landsat 8 images, including thermal channels B10 (10.60-11.19 microns) and B11 (11.50-12.51 microns). To obtain data on the thermodynamic temperature, Formula 1 was used:

$$T = \frac{K_2}{\ln\left(\frac{K_1}{R} + 1\right)} - 273,15 \quad (1)$$

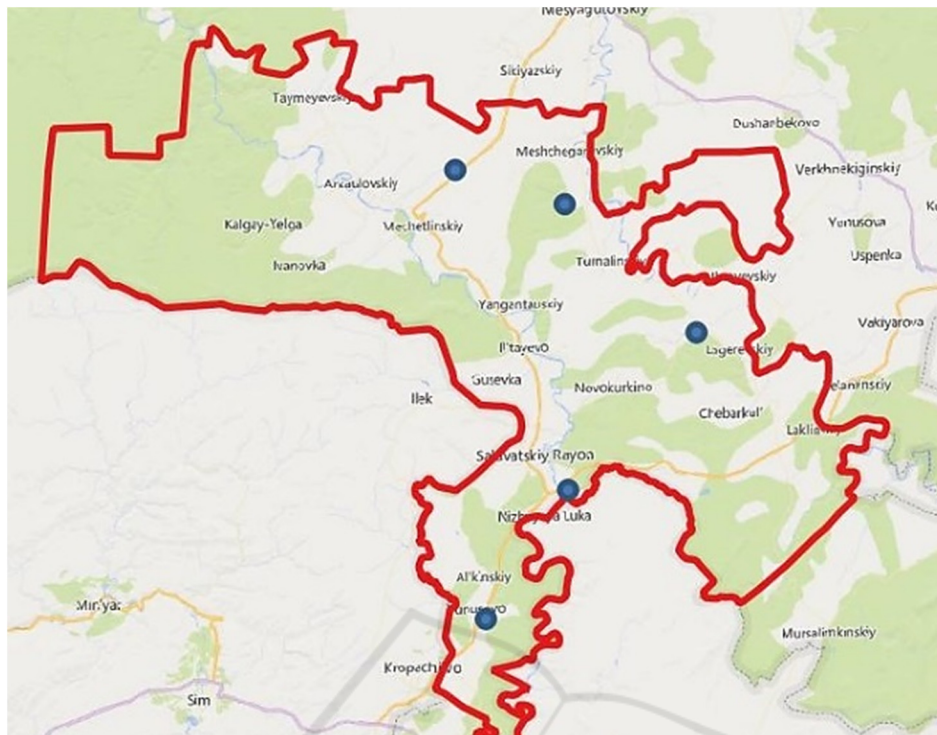


Figure 2: Locations of data loggers on the territory of the Yangan-Tau UNESCO global Geopark.

where  $T$  is the thermodynamic temperature, °C;  $K_1$  and  $K_2$  are calibration constants, the values of which are presented in Table 1.

Table 1: Calibration coefficients for Landsat 8 images.

Calibration coefficient	Channel B10	Channel B11
$K_1$	774.9	480.9
$K_2$	1321.1	1201.1
$M_R$	3,3420E-0,4	3,3420E-0,4
$A_R$	0.1	0.1

Further, according to the Formula (2), the  $R$  – intensity of the radiation of the object is calculated:

$$R = M_R * Q + A_R \quad (2)$$

where  $M_R$  and  $A_R$  are the calibration coefficients, the value of which is shown in Table 1;  $Q$  is the discrete calibrated pixel value.

The value of the calibration coefficients is presented in a meta-data file named "\*\_mtl.txt", included in the snapshot archive.

16 cloudless images were selected for analysis in the period from November 2020 to November 2021.

For the pixels corresponding to the location of the data loggers, the thermodynamic temperature values were calculated based on the formulas presented above. At the same time, the Q-GIS program has a

module for semi-automatic classification of the Earth's surface (Semi-Automatic Classification Plugin), which automatically recalculates the thermodynamic temperature. A comparison of the results obtained by calculation and the results obtained using the semi-automatic classification module showed their identity (Figure 3).

The correlation coefficient  $R$  for both channels was 0.99,  $R^2$  was 0.99, and the standard error was 0.55.

The temperature values determined by channels B10 and B11 (they differ in the covered intervals of the thermal range) of Landsat 8 differ from each other by 1.5-3 °C. In a number of publications, they are offered to average (Silkin, 2015).

### 3 RESULTS AND DISCUSSION

A regression analysis was carried out based on the data obtained from the images and data loggers. Both the entire range of annual results and seasonal results are analyzed. As can be seen in Figure 4 and Table 2, a correlation is observed during the year between the results obtained by ground measurements and data from Landsat 8 images.

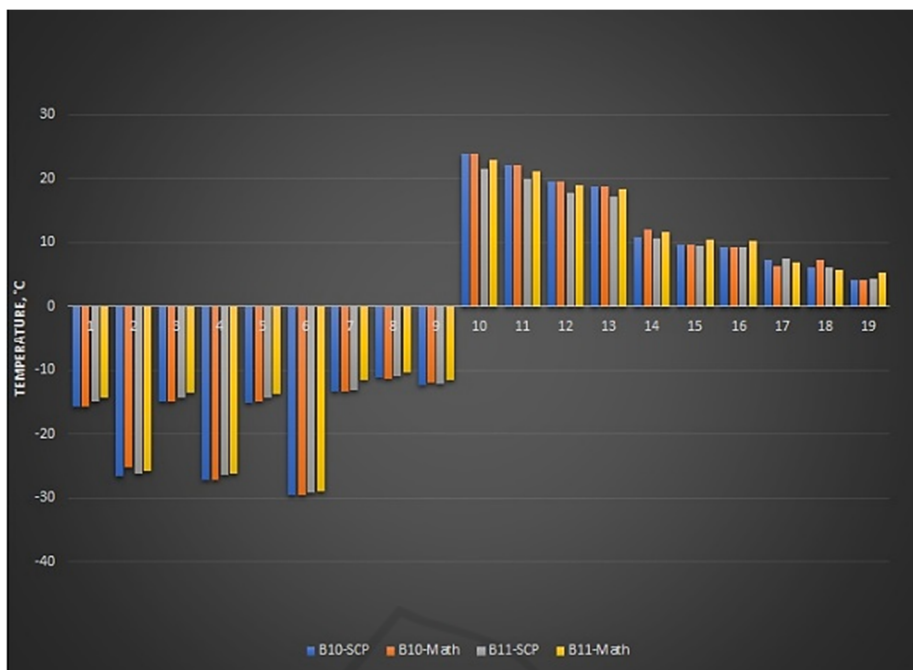


Figure 3: Comparison of calculation results and processing data in the Semi-Automatic Classification Plugin module, where B10-SCP and B11SCP are data obtained by processing in the Semi-Automatic Classification Plugin module for channels B10 and B11; B10-Math and B11-Math are data obtained by mathematical calculations.

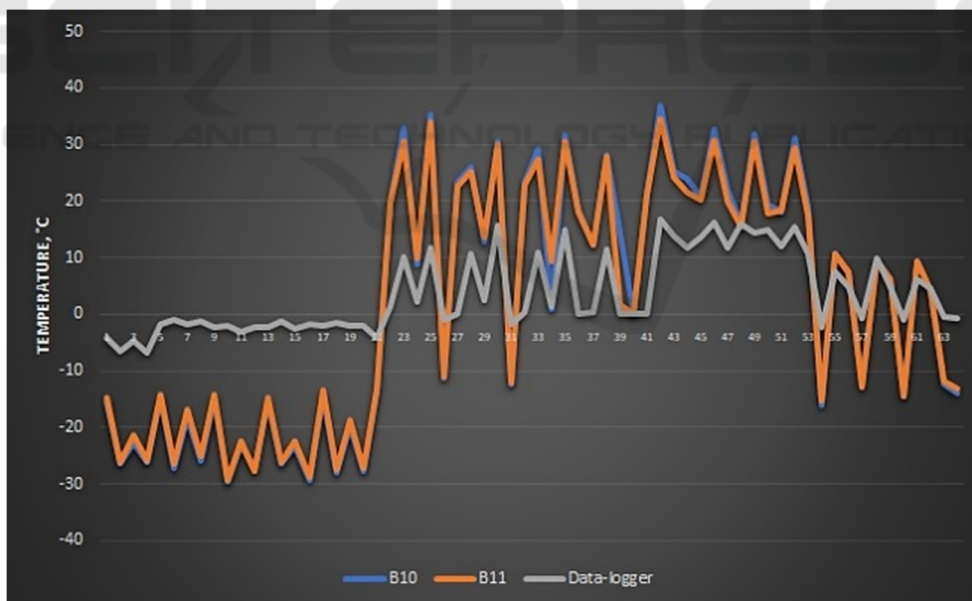


Figure 4: Temperature values from data loggers and Landsat 8 images.

At the same time, the analysis of seasonal data showed that there is no relationship between logger data and winter images (Figure 5), which is explained by the presence of snow cover (Table 2). The greatest correlation was observed in the autumn period (Figure 6).

As can be seen from Table 2, there are no significant differences in the correlation relationships between the results of ground measurements and the data of channels B10, B11 and their average values. In further studies, we used the average value of these channels B10 and B11.



Table 2: Relationships between ground-based research results and satellite data.

Period	Indicator	R	R <sup>2</sup>	Standard error
Year	B10	0.84	0.71	3.80
	B11	0.84	0.70	3.80
	AVG	0.84	0.71	3.80
Winter	B10	0.02	4,00E-04	1.68
	B11	0.02	4,00E-04	1.68
	AVG	0.02	4,00E-04	1.68
Spring	B10	0.76	0.58	4.10
	B11	0.77	0.59	4.00
	AVG	0.77	0.59	4.00
Summer	B10	0.55	0.31	1.77
	B11	0.57	0.33	1.75
	AVG	0.57	0.32	1.76
Autumn	B10	0.96	0.93	1.15
	B11	0.96	0.92	1.18
	AVG	0.96	0.93	1.16



Figure 5: Temperature values from data loggers and Landsat 8 images in winter.

Based on the data obtained, a linear predictive model of the relationship between data from Landsat 8 satellite images and the results of measurements by data loggers of soil temperature (Formula 3) is formulated:

$$T_{\text{soil}} = 3,06 + 0,28T_{\text{image}} \quad (3)$$

where  $T_{\text{soil}}$  is the soil temperature;  $T_{\text{image}}$  is the value of the thermodynamic temperature obtained from Landsat 8 images.

More accurate values can be obtained in the autumn period using other values of correction coefficients (Formula 4):

$$T_{\text{soil}} = 3,60 + 0,35T_{\text{image}} \quad (4)$$

## 4 CONCLUSIONS

1. To obtain the values of the thermodynamic surface temperature, you can use the Semi-automatic classification plugin of the QGIS program.
2. The use of satellite data for the winter period to assess soil temperature is not advisable, because snow cover has a significant impact on the temperature regime of the soil.
3. The greatest correlation between the satellite survey data and the results of ground

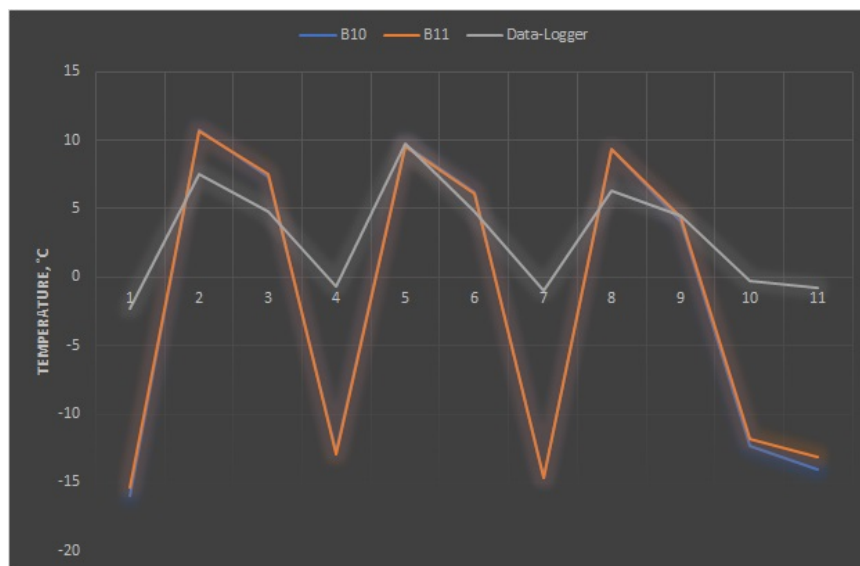


Figure 6: Temperature values from data loggers and Landsat 8 images in autumn.

measurements is observed in the autumn period.

- Remote data can be obtained as a result of processing channels B10, B11 or their average value. There are no differences in the relationship with ground data.

## ACKNOWLEDGEMENTS

The research was started with the assistance of the Russian Geographical Society, continued with the support of a grant from the Republic of Bashkortostan, the internal cipher of the scientific topic is ENOC-GVU-01-22.

## REFERENCES

- Jentsch, A., Beierkuhnlein, C., 2008. Research frontiers in climate change: Effects of extreme meteorological events on ecosystems. *Geoscience*. 340. 9-10. pp. 621-628.
- Larjavaara, M., Lu, X., Chen, X., Vastaranta, M., 2021. Impact of rising temperatures on the biomass of humid old - growth forests of the world. *Carbon Balance and Management*. Springer International Publishing. 31, 16. pp. 1-9.
- Thuiller, W. Albert, C., Araujo, M., Berry, P., Cabeza, M., Guisan, A., Hickler, T., Midgely, G., Paterson, J., Schurr, F., Sykes, M., Zimmermann, N., 2008. Predicting global change impacts on plant species' distributions: future challenges. *Perspectives in Plant Ecology, Evolution and Systematics*. 9, 3-4. pp. 137-152.
- Yuste, J., Baldocchi, D., Gershenson, A., Goldstein, A., Misson, L., Wong, S., 2007. Microbial soil respiration and its dependency on carbon inputs, soil temperature and moisture. *Global Change Biology*. 13. pp. 2018-2035.
- Hamdi, S., Moyano, F., Sall, S., Bernoux, M., Chevallier, T., 2013. Synthesis analysis of the temperature sensitivity of soil respiration from laboratory studies in relation to incubation methods and soil conditions. *Soil Biology and Biochemistry*. 58. pp. 115-126.
- Kravchenko, I. K., Tikhonova, E. N., Ulanova, R. V., Menko, E. V., Sukhacheva, M. V., 2019. Effect of temperature on litter decomposition, soil microbial community structure and biomass in a mixed-wood forest in European Russia. *Current Science*. 116, 5. pp. 765-772.
- El Garouani, M., Amyay, Mh., Lahrach, A., Oulidi, H. J., 2021. Land Surface Temperature in Response to Land Use/Cover Change Based on Remote Sensing Data and GIS Techniques: Application to Saïss Plain, Morocco. *Journal of Ecological Engineering*. 22, 7. pp. 100-112.
- Mamash, E. A., Pestunov, I. A., Chubarov, D. L., 2021. Construction of temperature maps of the city of Novosibirsk based on Landsat 8 satellite data. *Interexpo Geo-Siberia*. 4, 1. pp. 52-59.
- Kuular, H. B., 2018. The temperature of the landscape surface of the Republic of Tyva according to the Landsat-8 satellite in winter 2014-2017. *Modern problems of remote sensing of the Earth from space*. 15. 7. pp. 67-77.
- Kamalova, R. G., Belan, L. N., Bogdan, E. A., 2021. The climate of the Yangan-Tau Geopark and its modern changes. *Dynamics and interaction of the Earth's geospheres*. II. pp. 134-137.

- Perevedentsev, Yu. P., Vereshchagin, M. A., Shantalinsky, K. M., Naumov, E. P., Khabutdinov, Yu. G., 2011. *Changes in climatic conditions and resources of the Middle Volga region: a textbook on regional climatology*. p. 296.
- Silkin, K., 2015. *Correction of Landsat materials*. p. 5  
<https://gis-lab.info/qa/landsat-data-correction.html>.

